Chinese Traditional Medical Journal

A Comprehensive Metabolite Profiling Approach Utilizing In vivo Metabolic Reaction-Based Mass Difference Screening with Ultra-High-Performance Liquid Chromatography and Quadrupole-Time-of-Flight Mass Spectrometry for the Huangqi-Danshen Herb Pair

S. Venkatesh, A. Meghana

[1,2] Academy of Acupuncture and Moxibustion, Fujian University of Traditional Chinese Medicine, Fuzhou, Fujian 350122, China

Received on: 21 Jan 2025 Revised on: 20 Mar 2025 Accepted Date: 25 April 2025
Published on: 18 May 2025

Abstract: The goal of studying traditional Chinese medicine is to determine the biological roles played by the absorbed metabolites and prototypes in living organisms. However, due to endogenous interference and low metabolite abundance, complete in vivo component profiling is challenging. Thus, a methodical approach was suggested for the systematic screening and profiling of external components in biological matrices, using the mass differences between prototypes and their metabolic reaction products as a basis. Research Tools and Procedures: An extensive database based on metabolic reactions was constructed by collecting 247 metabolic reactions from the relevant literature on the Huangqi-Danshen (HD) herb pair. The mass differences were automatically computed using R programming and compared with the database in order to screen candidate components using the preprocessed data from experimental MS1 that was based on ultra-high-performance liquid chromatography combined with quadrupole-time-of-flight mass spectrometry. The components were then identified across the MS2 dataset. After oral administration of HD, 164 components were noted in the plasma samples of the rats. Out of them, 20 were validated using the reference standards. Amino acid dehydration, methylation, cysteine S-binding, glucuronidation, sulfation, and multistep reactions are prominent metabolic processes. Final Thoughts: This research paved the way for future studies to clarify HD's therapeutic benefits by revealing its metabolic features and biotransformation regulation. Beneficial tools for assessing metabolites in complex systems are provided by the suggested method.

INTRODUCTION

Traditional Chinese medicines (TCMs) and their related biological roles may be better understood by examining how they are metabolized in complex systems. The absorbed prototype components may undergo metabolic processes to generate their equivalent metabolites in vivo after oral treatment [1]. Metabolic profiling of TCMs is still difficult, nonetheless, due to their complex molecular make-up and unique biological changes. the third The quantities of exogenous prototypes or their metabolites are often at trace levels and are readily disguised by background interference, in contrast to endogenous metabolites in biological matrices. [4]

Due to its broad application, high sensitivity, high mass accuracy, and plentiful fragment information, liquid chromatography coupled with high-resolution mass spectrometry has been extensively used for metabolic profiling of exogenous substances. Five, six Researches have devised typical methods for analyzing MS data, including diagnostic ion filtering, manual annotation with mass defect filtering, neutral loss filtering, and quick mining of exogenous components of biological matrices. Another technique to effectively annotate possible chemicals in complicated matrices is to build an internal database that matches the biotransformation rules of the chemicalome and metabolome using published metabolic pathways as templates. [10] Data analysis becomes tedious, time-consuming, and prone to errors due to the vast and repeated human procedures required by these methodologies. Optimal MS parameterization, preprocessing of raw data, and automated database creation have all been accomplished using programming tools like R, Python, and Java. on pages 11 and 12, An effective strategy for in vivo metabolic profiling is to construct feature extraction rules based on metabolic reactions during ultra-high-performance liquid chromatography combined with quadrupole-time-of-flight mass spectrometry (UHPLC-QTOF MS) analysis. References [13,14]:

The constituents of the herb pair Huangqi-Danshen (HD), which includes Astragalus membranaceus (Fisch.) Bge. var. mongholicus (Bge.) Hsiao (Huangqi) and Salvia miltiorrhiza Bge. (Danshen), have been thoroughly studied in a preliminary study. These components primarily include phenolic acids, flavonoids, diterpenoids, and triterpenoids. However, the effects of these compounds in vivo remain unknown. By comparing the masses of metabolic reaction products and prototypes, we were able to devise a methodical approach to characterizing the exogenous components in rat plasma after oral HD treatment. We built a database after first collecting metabolic responses from the literature, then determining the mass changes between the prototype and the final result. Secondly, an ion list, containing RT and m/z values, was generated by preprocessing the full-scan MS1 data. After that, we used R to load the ion list and then used the mass differences to filter for potential components. The MS2 data on neutral losses, fragmentation modes, and diagnostic ions were used to further speculate or annotate the prototypes and their metabolites. We anticipated that this approach would provide HD in vivo metabolites, which would then serve as a reference for metabolic profiling of exogenous substances in TCMs and as a foundation for future studies on the pharmacodynamic basis and pharmacological processes.

Plasma sample and simulated biological sample preparation

Materials and Methods

Chemicals and reagents

Methanol and acetonitrile (HPLC-grade) were purchased from Merck (Darmstadt, Germany). Analytical ethanol was purchased from Shanghai Titan Technology Co. Ltd. (Shanghai, China). Formic acid was supplied by ROE Company (Newark, USA). Isoflurane was supplied by Shenzhen Rivard Life Technology Co. Ltd. (Shenzhen, China). Heparin sodium was supplied by Shanghai Yuanye Biotechnology Co. Ltd. (Shanghai, China). Ultrapure water was prepared using a Milli-Q water purification system (Millipore, Billerica, MA, USA).

The *A. membranaceus* (Fisch.) Bge. var. *mongholicus* (Bge.) Hsiao was collected from Wulanchabu (Inner Mongolia, China), while *S. miltiorrhiza* Bge. was obtained from Linyi (Shandong, China). The herbal components were identified by Professor Hua Yang. A total of 76 chemical reference standards (purity > 95%) were used in this study, including 22 phenolic acids, 17 flavonoids, 19 diterpenoids, 13 triterpenoid saponins, and 5 others.

Standard solution and huangqi-danshen samples preparation

The *A. membranaceus* (Fisch.) Bge. var. *mongholicus* (Bge.) Hsiao and *S. miltiorrhiza* Bge. were mixed in a ratio of 1:1 (*w*/*w*) and soaked in 50% ethanol (1:10, *w*/*v*) for 30 min, followed by extraction under reflux for 2 h twice. The extracted samples were mixed and concentrated under the vacuum using a rotary evaporator. Then, the concentrated extract was lyophilized and stored at 4°C. The lyophilized HD powder was dissolved in 1.5 g/mL saline before administration. The standard was dissolved in methanol (1.0 mg/mL) to obtain a single stock solution.

Animal experiments

All animal experiments were performed in compliance with the Guidelines for Pharmaceutical Animal Experiments of the China Pharmaceutical University (No. 2022-03–047). Ten male Spraque-Dawley rats (220 ± 20 g) were obtained from Vital River Laboratory Animal Technology Co., Ltd. (Zhejiang, China). The animals were kept in a constant chamber with a 12-h photoperiod, relative humidity (50 ± 5%), and temperature (25°C ± 2°C). They were allowed to eat and drink freely for 7 days to acclimatize. Before drug administration, all rats were allowed to drink freely for 12 h.

The rats were randomly divided into HD and control groups. The HD group rats were administered by gavage at 6.25 g/kg, whereas the control group rats were administered normal saline. Blood samples were retrieved from ophthalmic veins using heparinized tubes at 0 (predose), 5, 15, 30 min, 1, 2,
4, 6, 8, 10, 12, and 24 h. Immediately centrifuged the blood sample at 3000 rpm for 10 min at 4°C. The supernatant plasma at the same time point in rats was mixed in equal volumes and immediately stored at -80°C until analysis.

After thawing on the ice, 90 μL plasma samples were mixed with 360 μL cold acetonitrile. The mixture was vortexed for 3 min and centrifuged at 13,000 rpm for 15 min at 4°C. The supernatant was collected and dried using an EZ-2 Personal Evaporator (GeneVac, UK). The metabolite extract was then dissolved in 90 μL acetonitrile/water mixture (1:1, v/v), swirled for 3 min, and then centrifuged at 13,000 rpm at 4°C for 10 min before analysis.

For the simulated biological sample, 120 μL aliquots of blank plasma sample were placed to four 1.5 mL microcentrifuge tubes in equal parts after thawing on the ice. The obtained samples were mixed with cold acetonitrile (1:4, v/v), swirled for 3 min, and centrifuged at 13,000 rpm at 4°C for 15 min. The supernatant was collected in a microcentrifuge tube and dried using the EZ-2 Personal Evaporator. To distinguish the isomeric reference materials, single reference material solutions were divided into four groups. The standard solution of each group was taken 5 μL and prepared into 120 μL mixed solution. The metabolite extract was reconstituted in the mixed solution and centrifuged at 13,000 rpm for 15 min at 4°C after being vortexed for 3 min. The resulting supernatant was transferred to a sampling vial for UHPLC-QTOF MS.

Ultra-high-performance liquid chromatography coupled with quadrupole-time-of-flight mass spectrometry analysis

Detection was conducted using an Agilent 6530 quadrupole time-of-flight mass spectrometer connected to an Agilent 1290 UHPLC (Agilent Technologies Inc., California, US). A Waters ACQUITY UPLC HSS T3 column (2.1 mm × 100 mm, 1.8 μm, US) was utilized at a column oven temperature of 35°C for chromatographic separation. The mobile phase made up of 0.1% (*v*/v) aqueous formic acid (phase A) and acetonitrile (phase B). The mobile phase gradient program was: 0–2 min, 5%–20% B; 2–7 min, 20%–35% B; 7–9 min, 35%–50% B; 9–12 min, 50%–53% B; 12–18 min, 53%–60% B; 18–21 min, 60%–80% B; 21–24 min, 80%–95% B; 24–30 min, 95% B while the posttime was 5 min. The volume injected was 2 μL and flow rate was set to 0.3 mL/min.

The mass spectrometric parameters were set as follows: drying gas, nitrogen; gas flow rate, 10 L/min; gas temperature, 350°C; nebulizer pressure, 35 psi; sheath temperature, 350°C; sheath gas flow, 11 L/min; electrospray capillary voltage, 4000 V in the positive mode and 3500 V in the negative mode; fragment voltage, 135 V; skimmer voltage, 65 V; octopole RF peak, 750 V; mass range, MS: 100–1500 m/z, MS/MS: 50–1500 m/z; and collision energy, 10, 20, 30, 40, 50, and 60 eV. Mass spectrometry was conducted in the positive and negative ion modes. To prove the accuracy of mass spectrometry detection, the mass axis was calibrated by tuning the liquid before daily injection analysis.

Database construction

Through retrieving the relative literatures from PubMed (https://pubmed.ncbi.nlm.nih.gov/) and Google scholar (https://scholar.google.com/) using the keywords "*Astragalus membranaceus* (Fisch.) Bge. var. *mongholicus* (Bge.) Hsiao, Huangqi, *Salvia miltiorrhiza* Bge., Danshen, Metabolites." We collected the related metabolic reactions and drug components *in vivo* and organized the substituents created or lost during the metabolic reactions. Moreover, we manually recorded information on the mass differences created during the metabolic reactions. The database contains information on reaction names, formula changes, mass differences, classifications, and citations.

Data processing

Raw MS^1 data for the blood samples were processed using Profinder B.10.0 (Agilent Technologies, USA). First, the data for HD group and control group were grouped according to the positive ion mode or negative ion mode with peak height ≥100 counts. The adduct ions of positive ions were $[M + H]^+$, $[M + Na]^+$, and negative ions were $[M-H]^-$, $[M + Cl]^-$, $[M + HCOO]^-$. An isotope model was set for common organic compounds (no halogens). Other parameters were as follows: limit assigned charge states to a maximum of 1; RT window = 0.00% +0.4 min; mass window = 25 ppm + 2.0 mDa; compound ion count threshold ≥ 2. The EIC tolerance was set at ± 35.0 ppm and the RT was ± 1.5 min. The ion lists were then exported to Microsoft Excel files (. csv), which contained key information such as RT and mass.

R-assisted candidate components screening

For the rapid screening of candidate components in the bio-samples, *R* programming (version 4.0.2) was used to develop the code. The ion lists were imported into the *R* programming to automatically calculate the mass differences between each pair of ions in the list to screen more candidate components. The mass differences between the experimental feature ions and the database were manually compared, and the candidate ions with mass error within ± 10 ppm were collected for further research.

RESULTS

The establishment of a systematic strategy

A systematic strategy was developed to screen and analyze the exogenous components in biological matrices using the following procedure [Figure 1]. First, the raw MS^1 data were preprocessed using Profinder 10.0 software to generate ion lists, which included RT and mass values for detected components. Second, a mass-difference database containing information on the biotransformation rules of the components was built to screen the metabolites *in vivo*. The mass differences between the experimental ions were calculated automatically using *R* programming, and the values were screened by matching them with the database. Subsequently, a mass error within 10 ppm was included for the candidate components. Finally, the prototype and metabolite constituents in the plasma were annotated and

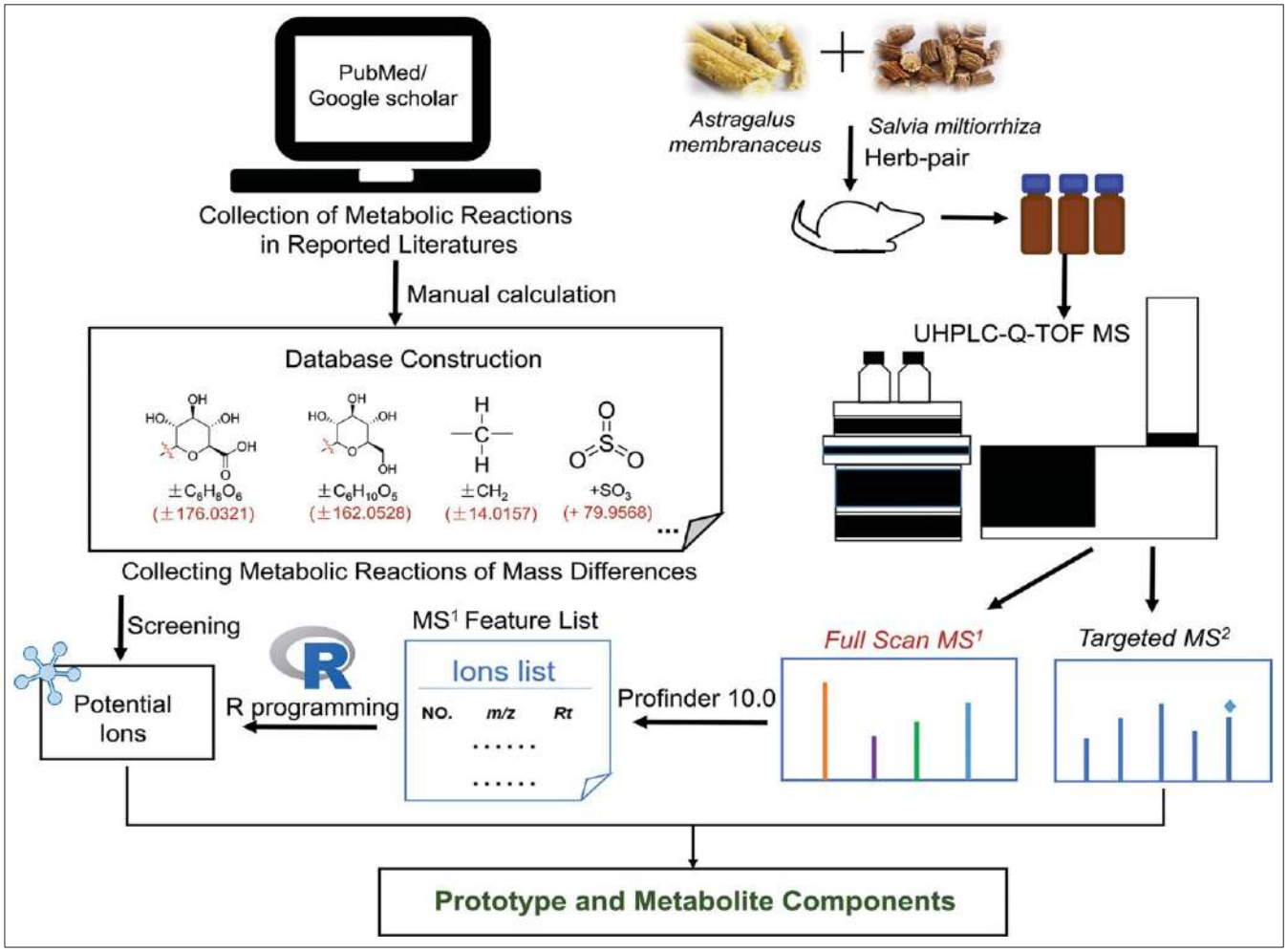

Figure 1: The schematic diagram of the comprehensive strategy

identified according to literature, reference standards, and MS^2 information.

Database for metabolic reaction of mass difference in huangqi-danshen

For drug compounds *in vivo*, a metabolic reaction of the mass difference database was established based on the prototypes and metabolites to screen feature ions quickly and effectively. By searching the reference literature from PubMed and Google Schola, 46 studies related to the identification of components of HD and related components *in vivo* were identified and organized. A total of 247 metabolic reactions were collected and the mass difference of each metabolic reaction was calculated manually.

Database combined with *R* programming for screening of candidate components

Profinder 10.0 was used to extract 862 positive and 976 negative ions from the original MS^1 information. The feature ion lists were imported into the *R* programming to automatically calculate the mass difference between different ions. Then, the mass difference of each feature ion pair was matched with the database, and the ions pair of mass error within ± 10 ppm was collected as the candidate components. Consequently, 485 positive and 566 negative ions were efficiently screened as potential HD-related candidates.

Identification the absorbed prototypes and metabolites of huangqi-danshen

To identify the candidate HD components, MS^2 data were collected for further analysis based on diagnostic ions, neutral losses, reference substances, and literature reports. The total ion chromatograms of rat plasma after oral HD treatment are shown in Figure 2. A total of 164 compounds, including 90 prototypes and 74 metabolites, were explicitly or presumably identified in this study. The compounds included 49 flavonoids, 28 phenolic acids, 84 terpenoids, and 3 others. Tables 1 and 2 display the detailed information.

Identification of flavonoids

Flavonoids are the main components of Huangqi and can be further divided into flavones, isoflavones, flavanones, and flavonols.[16] They have many pharmacological activities such as promoting osteogenic function, improving liver cell dysfunction, and exerting anti-inflammatory effects.[17-19] In

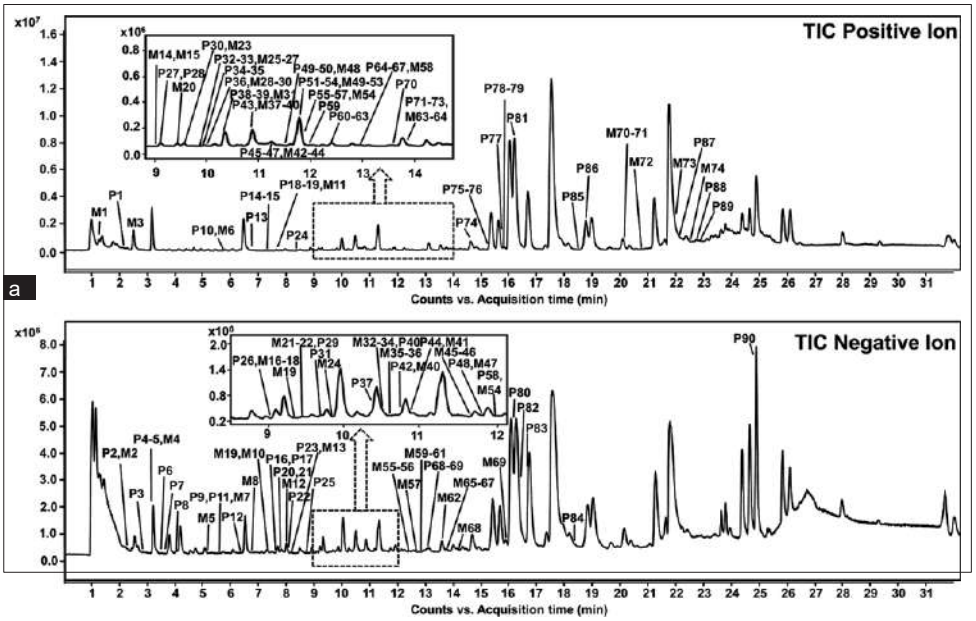

Figure 2: Total ion chromatograms in positive (a) and negative (b) mode in rat plasma after oral administration of Huangqi-Danshen

this study, 49 flavonoids were annotated as HD, including 27 prototypes and 22 metabolites.

The component P22 ($C_{16}H_{12}O_5$) generated an $[M-H]^-$ ion at m/z 283.0604, which produced fragment ions at m/z 239.0509 ($[M-H-CO]^-$), 237.0535 ($[M-H-OCH_2-O]^-$), and 225.0175 ($[M-H-CO-CH_2]^-$). Compared to the standard reference, P22 was confirmed to be calycosin. In addition, P37 showed an $[M-H]^-$ ion at m/z 267.0690 and an $[M+H]^+$ ion at m/z 269.0804, with the same formula as $C_{16}H_{12}O_4$. P37 exhibited ions at m/z 252.0450 ($[M-H-CH_3]^-$), 223.0396 ($[M-H-CO_2]^-$), 208.0578 ($[M-H-CH_3-CO]^-$), and 137.0418 (*Retro Diels-Alder reaction, RDA reaction*), which were determined to be formononetin using a standard reference.

Metabolite M7 ($C_{22}H_{23}NO_8S$) showed a parent ion at m/z 460.1088 $[M-H]^-$, and the product ions were generated at m/z 283.0624 and 239.0174 matched those of P22. Compared to the literature, M7 was identified as the metabolic product of P22, which is involved in di-hydrogenation and cysteine S-binding.[20] Metabolite M8 ($C_{22}H_{20}O_{10}$, m/z 443.1012, $[M-H]^-$) was eluted at 6.98 min and its product ions at m/z 267.0761 ($[M-H-C_6H_8O_6]^-$), 252.0563 ($[M-H-C_6H_8O_6-CH_3]^-$) and 208.0438 ($[M-H-C_6H_8O_6-CH_3-CO_2]^-$), showing the same MS^2 fragmentation pattern with P37. Therefore, M8 suggested the presence of $C_6H_8O_6$, which increased by 176 Da relative to formononetin [Figure 3]. Metabolite M30 (*m/z* 283.0958, $[M+H]^+$) was 14 Da higher than that of P37, showing the same product ions at m/z 268.0954 and 239.0952 connected with $[M+H-CH_3]^+$ and $[M+H-CO]^+$. Therefore, M30 may be the methylation product of P37. Figure 4 shows the potential flavonoid metabolic pathways, including glucuronidation, methylation, cysteine S-conjugation, and hydrogenation.

Identification of phenolic acids

Phenolic acids, which mainly originate from Danshen, provide anti-inflammatory, anti-oxidant, anti-thrombotic, and other pharmacological effects.[21-23] Salvianolic acid compounds contain danshensu or caffeic acid in their basic structure, forming different dimers, trimers, tetramers, and salt derivatives.[24] In this study, 28 compounds were characterized in the plasma samples, consisting of 14 prototypes and 14 products.

Compound P8 generated a molecular formula of $C_9H_{10}O_5$ and exhibited $[M-H]^-$ ion at *m/z* 197.0472. The MS^2 characteristic information at *m/z* 169.0313, 165.0652, 153.0233, and 151.0067 correspond to $[M-H-CO]^-$, $[M-H-2O]^-$, $[M-H-CO_2]^-$, and $[M-H-H_2O-CO]^-$, respectively. P8 was confirmed to be danshensu by comparison with a standard reference. Moreover, the prototype compounds P4 and P12 were characterized as protocatechuic and rosmarinic acids, respectively, based on comparison with the characteristic ions of the standards.

Metabolite M1 (*m/z* 211.0618, $[M+H]^+$) was 16 Da larger than ferulic acid, with a molecular formula of $C_{10}H_{10}O_5$. The product ions were observed at *m/z* 195.0588 ($[M+H-O]^+$) and 167.0735($[M+H-CO_2]^+$), which had the same characteristics as ferulic acid. Therefore, M1 was hypothesized to be the hydroxylation product of ferulic acid.[25] Metabolite M9 displayed an $[M-H]^-$ ion at *m/z* 273.0101, which was 62 Da higher than that of the parent danshensu, indicating the presence of sulfate group binding (+80 Da), methylation (+14 Da), and dehydration (-18 Da) reactions. The MS^2 fragment information for M9 at *m/z* 193.0821 and 229.0707 indicated the loss of SO_3 (80 Da) and CO_2 (44 Da), respectively. The fragmentation pathway is shown in Figure 5. In addition, this study mainly presents the metabolic reactions of related

Table 1: Identification of the prototype constituents of HD in plasma by UHPLC-QTOF MS

No.	RT (min)	*m/z*	Adducts	Formula	Theoretical *m/z*	Error (ppm)	Fragment ions	Identification	Structure Type
P1	2.23	341.0670	$[M+H]^+$	$C_{18}H_{12}O_7$	341.0656	4.10	297.0788, 282.0495	Salvianolic acid G	Phenolic acids
P2	2.49	581.1850	$[M+HCOO]^-$	$C_{26}H_{32}O_{12}$	581.1876	-4.44	417.1187, 353.1311, 374.0591,	1-Hydroxypinoresinol-1-*O*-*β*-*D*-glucoside	Phenolic acids
P3	2.92	313.0693	$[M-H]^-$	$C_{17}H_{14}O_6$	313.0712	-6.07	285.0179, 251.0431, 137.0239	4’,5-Dihydroxy-7,8-dimethoxyflavone	Flavonoids
P4*	3.17	153.0200	$[M-H]^-$	$C_7H_6O_4$	153.0193	4.36	135.0470, 123.0491, 109.0304	Protocatechuic acid	Phenolic acids
P5	3.17	239.0567	$[M+HCOO]^-$	$C_{10}H_{10}O_4$	239.0561	2.51	215.0708, 203.0922, 116.0545	Caffeic acid methyl ester	Phenolic acids
P6	3.55	211.0595	$[M-H]^-$	$C_{10}H_{12}O_5$	211.0612	-8.05	193.0578, 179.0236, 169.0763, 150.0375	Danshensu methyl ester	Phenolic acids
P7*	3.65	269.0807	$[M-H]^-$	$C_{16}H_{14}O_4$	269.0819	-4.58	203.0848, 175.0246, 147.0134, 93.0354	Medicarpin	Flavonoids
P8*	4.11	197.0480	$[M-H]^-$	$C_9H_{10}O_5$	197.0455	8.63	169.0313, 165.0652, 153.0233, 151.0067	Danshensu	Phenolic acids
P9	5.60	447.0973	$[M-H]^-$	$C_{21}H_{20}O_{11}$	447.0933	8.38	295.0582, 131.008	Kaempferol 3-*O*-*β*-*D*-glucoside	Flavonoids
P10	5.62	461.1041	$[M+H]^+$	$C_{22}H_{20}O_{11}$	461.1078	-8.11	285.0621, 71.0007	Wogonoside	Flavonoids
P11	5.63	461.1120	$[M-H]^-$	$C_{22}H_{22}O_{11}$	461.1089	6.65	177.0296, 85.0345	Hispiduloside	Flavonoids
P12*	6.44	359.0792	$[M-H]^-$	$C_{18}H_{16}O_8$	359.0767	5.46	302.1233, 283.0118, 235.0542	Rosmarinic acid	Phenolic acids
P13*	6.81	431.1329	$[M+H]^+$	$C_{22}H_{22}O_9$	431.1337	-1.76	369.0485, 271.0183, 269.0822, 241.0865,	Ononin	Flavonoids
P14	7.31	489.1383	$[M+H]^+$	$C_{24}H_{24}O_{11}$	489.1391	-1.71	257.0051, 237.0712	Calycosin 7-*O*-*β*-*D*-glucoside-6’’-*O*-acetate	Flavonoids
P15*	7.35	303.1218	$[M+H]^+$	$C_{17}H_{18}O_5$	303.1227	-2.97	285.1221, 199.0871, 125.0942, 107.0618	Isomucronulatol	Flavonoids
P16	7.57	479.1585	$[M-H]^-$	$C_{23}H_{28}O_{11}$	479.1559	5.46	303.0291, 301.0472	(3*R*)-7,2’-Dihydroxy-3’,4’-dimethoxyisoflavan-7-*O*-*β*-*D*-glucuronide	Flavonoids
P17	7.64	501.1085	$[M-H]^-$	$C_{24}H_{22}O_{12}$	501.1038	9.28	235.0739, 193.0568	Di-feruloyl-tartaric acid	Phenolic acids
P18	7.69	301.1036	$[M+H]^+$	$C_{17}H_{16}O_5$	301.1071	9.46	283.1046, 167.0715	(6a*R*,11a*R*)-3,9-Dimethoxy-10-hydroxypterocarpan	Flavonoids
P19	7.69	477.1378	$[M+H]^+$	$C_{23}H_{24}O_{11}$	477.1391	-2.80	300.1300, 269.0956, 167.0688, 145.0899	Odoratin 7-*O*-*β*-*D*-glucopyranoside	Flavonoids
P20	7.74	373.0950	$[M-H]^-$	$C_{19}H_{18}O_8$	373.0929	5.65	249.0125, 135.06	Methyl rosmarinate	Phenolic acids
P21	7.77	463.1640	$[M-H]^-$	$C_{23}H_{28}O_{10}$	463.1610	6.69	164.0442, 153.0659	2’-Hydroxy-3’,4’-dimethoxyisoflavan 7-*O*-*β*-*D*-glucoside	Flavonoids
P22*	8.01	283.0604	$[M-H]^-$	$C_{16}H_{12}O_5$	283.0612	-2.83	239.0509, 237.0535, 225.0175, 183.0146	Calycosin	Flavonoids
P23*	8.17	283.0635	$[M-H]^-$	$C_{16}H_{12}O_5$	283.0612	8.13	269.0679, 196.0774	Glycitein	Flavonoids
P24*	8.44	313.1076	$[M+H]^+$	$C_{18}H_{16}O_5$	313.1071	1.76	295.1090, 267.0986, 257.0920, 253.0872, 219.0855	Tanshindiol B	Diterpenoids
P25*	8.84	829.4600	$[M+HCOO]^-$	$C_{41}H_{68}O_{14}$	829.4591	1.07	785.1802, 489.4880, 315.6395	Isoastragaloside IV	Triterpenoids
P26	9.11	487.1263	$[M-H]^-$	$C_{24}H_{24}O_{11}$	487.1246	3.49	311.022, 145.0784	6’’-*O*-Acetylglycitin	Flavonoids
P27	9.32	295.0956	$[M+H]^+$	$C_{18}H_{14}O_4$	295.0965	-3.00	277.0777, 267.0653, 259.0777, 251.0746	Trijuganone A	Diterpenoids
P28	9.39	313.1061	$[M+H]^+$	$C_{18}H_{16}O_5$	313.1071	-3.03	299.1282, 297.1072, 267.1042, 205.0338	Tanshindiol A	Diterpenoids
P29	9.57	299.0919	$[M-H]^-$	$C_{17}H_{16}O_5$	299.0925	-2.00	269.0774, 255.0559	3-Hydroxy-4,9-dimethoxypterocarpan	Flavonoids

Contd...

Table 1: Contd...

No.	RT (min)	*m/z*	Adducts	Formula	Theoretical *m/z*	Error (ppm)	Fragment ions	Identification	Structure Type
P30	9.69	313.1431	$[M+H]^+$	$C_{19}H_{20}O_4$	313.1434	-1.07	297.1280, 295.1333, 285.1468, 271.1060	3-Hydroxycryptotanshinone	Diterpenoids
P31	9.70	285.1515	$[M-H]^-$	$C_{18}H_{22}O_3$	285.1496	6.66	241.1436, 229.1076, 167.0387	Przewalskin F	Diterpenoids
P32	9.91	313.1403	$[M+H]^+$	$C_{19}H_{20}O_4$	313.1434	-9.90	298.1101, 269.1509, 257.1604, 255.1087	Miltionone I	Diterpenoids
P33	9.92	311.1258	$[M+H]^+$	$C_{19}H_{18}O_4$	311.1278	-6.38	297.1137, 267.1361, 253.0781, 147.0768, 57.0704	Hydroxytanshinone	Diterpenoids
P34	9.99	293.1147	$[M+H]^+$	$C_{20}H_{20}O_3$	293.1172	-8.60	275.1185, 219.0843	Dehydrotanshinone	Diterpenoids
P35	9.99	325.1415	$[M+H]^+$	$C_{10}H_{13}O_5$	325.1434	-5.96	215.0817, 211.1118, 165.0656	(*S*)-5,7-Dihydroxy-6-prenylflavanone	Flavonoids
P36	10.00	284.0967	$[M+H]^+$	$C_{16}H_{12}NO_4$	284.0989	-7.74	238.0934, 136.0534, 135.1183, 107.0564	Guanosine	Others
P37*	10.39	267.0690	$[M-H]^-$	$C_{16}H_{12}O_4$	267.0663	9.18	252.0450, 223.0369, 208.0578, 137.0418	Formononetin	Flavonoids
P38	10.46	293.0821	$[M+H]^+$	$C_{17}H_{16}O_3$	293.0808	4.32	265.0849, 249.0946	Tanshinol A	Diterpenoids
P39	10.47	269.1183	$[M+H]^+$	$C_{16}H_{16}O_5$	269.1172	4.01	251.1073, 233.0999, 223.1110, 205.1021	Epidanshenspiroketallactone	Diterpenoids
P40	10.49	287.0956	$[M-H]^-$	$C_{17}H_{18}O_3$	287.0925	9.81	269.1250, 259.0922, 243.1326	(3*R*)-7,2',3'-Trihydroxy-4'-methoxyisoflavane	Flavonoids
P41	10.70	271.1335	$[M+H]^+$	$C_{18}H_{14}O_4$	271.1329	2.32	259.0857, 197.0723, 179.0898	Neocryptotanshione II	Diterpenoids
P42	10.72	377.0792	[M+Cl]-	$C_{19}H_{18}O_6$	377.0797	-1.33	311.0899, 297.0931, 249.0577, 243.0766	Tanshinoic acid B	Phenolic acids
P43	10.76	295.0960	$[M+H]^+$	$C_{18}H_{18}O_4$	295.0965	-1.69	277.0852, 251.0577, 237.0527, 209.0597	3α-Hydroxymethylenetanshinquinone	Diterpenoids
P44*	10.82	283.0605	$[M-H]^-$	$C_{16}H_{12}O_5$	283.0612	-2.47	253.0364, 237.0669	Wogonin	Flavonoids
P45	11.14	317.1403	$[M+H]^+$	$C_{18}H_{16}O_4$	317.1384	6.15	301.1504, 299.1252, 285.1503, 271.1363	7-*O*-methylisomucronulatol	Flavonoids
P46	11.15	297.1131	$[M+H]^+$	$C_{18}H_{18}O_4$	297.1121	3.25	279.1019, 265.1266, 261.0932, 233.0946, 179.0867	Tanshinol B	Diterpenoids
P47	11.24	315.1217	$[M+H]^+$	$C_{18}H_{18}O_5$	315.1227	-3.17	297.1102, 279.1140, 271.1292, 147.0778	15,16-Dihydrotanshinol B	Diterpenoids
P48	11.78	453.1319	[M+Cl]-	$C_{22}H_{26}O_8$	453.1322	-0.66	399.1609, 181.0615, 137.0081	Syringaresinol	Others
P49	11.79	359.1421	$[M+H]^+$	$C_{22}H_{18}N_2O_3$	359.1390	8.63	342.1324, 341.1469, 311.1269	Isosalviamides G	Diterpenoids
P50	11.80	297.1483	$[M+H]^+$	$C_{19}H_{20}O_3$	297.1485	-0.74	271.1349, 249.1057, 211.0768	Isocryptotanshinone	Diterpenoids
P51	11.82	267.1367	$[M+H]^+$	$C_{18}H_{18}O_2$	267.1380	-4.87	253.1243, 249.1410, 239.1465, 224.0543	4-Methylenemiltirone	Diterpenoids
P52	11.82	287.1300	$[M+H]^+$	$C_{17}H_{18}O_4$	287.1278	7.71	269.1116, 233.1072, 181.0981	2'-Hydroxy-3', 4'-dimethoxyisoflavan	Flavonoids
P53	11.83	313.1428	$[M+H]^+$	$C_{19}H_{20}O_4$	313.1434	-1.92	123.1181, 267.1253, 295.1341, 297.1212	17-Hydroxycryptotanshinone	Diterpenoids
P54*	11.84	311.1286	$[M+H]^+$	$C_{19}H_{18}O_4$	311.1278	2.62	295.0989, 293.1124, 267.1372	Tanshinone IIB	Diterpenoids
P55	11.92	293.0797	$[M+H]^+$	$C_{18}H_{20}O_4$	293.0808	-3.75	249.0883, 178.0775	Monodydroxytanshinone I	Diterpenoids
P56	11.92	301.1446	$[M+H]^+$	$C_{20}H_{20}O_5$	301.1434	3.87	285.1441, 283.1330, 265.1307, 255.0993	Salvianonol	Diterpenoids
P57	11.96	341.1362	$[M+H]^+$	$C_{20}H_{24}O_6$	341.1389	-7.91	221.0972, 115.0953, 83.0277	Trijuganone C	Diterpenoids
P58	11.97	359.1506	$[M-H]^-$	$C_{18}H_{22}O_3$	359.1500	1.67	221.0972, 115.0953, 83.0277	Lariciresinol	Others
P59	12.03	287.1642	$[M+H]^+$	$C_{18}H_{22}O_3$	287.1642	0.10	271.1628, 269.1544, 261.1322, 251.1406, 231.1016	Cryptoacetalide	Diterpenoids

Contd...

Table 1: Contd...

No.	RT (min)	*m/z*	Adducts	Formula	Theoretical *m/z*	Error (ppm)	Fragment ions	Identification	Structure Type
P60	12.43	299.1981	$[M+H]^+$	$C_{20}H_{26}O_2$	299.2006	-8.21	284.1627, 255.1587, 253.1972, 241.1245	Microstegiol	Diterpenoids
P61	12.49	279.0991	$[M+H]^+$	$C_{18}H_{14}O_3$	279.1016	-8.85	267.1035, 265.0792, 233.0933, 221.0775	Methylenetanshinquinone	Diterpenoids
P62	12.49	301.0707	$[M+H]^+$	$C_{16}H_{12}O_6$	301.0712	-0.55	285.0849, 245.0820	3,3',7-Trihydroxy-4'-methoxyflavone	Flavonoids
P63	12.49	579.1719	$[M+H]^+$	$C_{27}H_{30}O_{14}$	579.1708	1.90	521.1344, 425.0752	Violanthin	Flavonoids
P64	12.93	309.1083	$[M+Na]^+$	$C_{17}H_{18}O_4$	309.1097	-4.53	223.0723, 165.0588, 139.0717	4'-Hydroxy-5,7-dimethoxyflavan	Flavonoids
P65	12.93	311.1249	$[M+H]^+$	$C_{19}H_{18}O_4$	311.1278	-9.27	297.1037, 295.1289, 283.0846, 237.1279	Isotanshinone IIB	Diterpenoids
P66	12.93	327.1199	$[M+H]^+$	$C_{19}H_{18}O_5$	327.1227	-8.56	309.1136, 283.1298, 265.1206, 223.0751	3-Hydroxytanshinone IIB	Diterpenoids
P67*	12.97	297.1116	$[M+H]^+$	$C_{18}H_{16}O_4$	297.1121	-1.8	281.1041, 279.1038, 263.0995, 251.1018, 233.1006	Danshenxinkun A	Diterpenoids
P68	13.01	295.0994	$[M-H]^-$	$C_{18}H_{16}O_4$	295.0976	6.10	277.1000, 249.0971, 237.0969	Tanshinone VI	Diterpenoids
P69	13.01	297.1123	$[M+HCOO]^-$	$C_{17}H_{16}O_2$	297.1132	-3.14	253.0741, 238.0611	Salyunnanin D	Diterpenoids
P70	13.67	517.1327	$[M+H]^+$	$C_{25}H_{24}O_{12}$	517.1341	-2.71	471.1302, 455.1270, 343.1491, 103.0473	Formononetin-7-*O*-*β*-*D*-glucoside-6"-*O*-malonate	Flavonoids
P71	13.85	355.1032	$[M+Na]^+$	$C_{14}H_{20}O_9$	355.1005	9.14	271.1145, 183.0568	Leonuriside A	Phenolic acids
P72	13.86	297.1474	$[M+H]^+$	$C_{19}H_{20}O_3$	297.1485	-3.77	269.1572, 253.1582, 237.0902, 211.1415	1-Oxomiltirone	Diterpenoids
P73	13.86	269.1539	$[M+H]^+$	$C_{18}H_{20}O_2$	269.1536	1.09	254.1205, 227.1181, 191.0002	Salvinone	Diterpenoids
P74*	14.86	279.0996	$[M+H]^+$	$C_{18}H_{14}O_3$	279.1016	-7.06	261.0978, 237.0809, 233.0947	Dihydrotanshinone I	Diterpenoids
P75	15.21	279.0986	$[M+H]^+$	$C_{18}H_{14}O_3$	279.1016	-9.46	261.0783, 233.0869, 221.0803	1,2-Dihydrotanshinquinone	Diterpenoids
P76	15.21	297.1138	$[M+H]^+$	$C_{18}H_{16}O_4$	297.1121	5.60	279.1019, 261.0961, 233.1056	Salmiltiorin A	Diterpenoids
P77	15.62	567.1486	$[M+H]^+$	$C_{29}H_{26}O_{12}$	567.1497	-1.94	225.0348, 184.0741, 135.0745	Ethyl lithospermate	Phenolic acids
P78*	15.70	281.1180	$[M+H]^+$	$C_{18}H_{16}O_3$	281.1172	2.77	263.1048, 248.0706, 235.1119, 220.0855	Trijuganone B	Diterpenoids
P79*	15.77	315.1561	$[M+H]^+$	$C_{19}H_{22}O_4$	315.1591	-9.52	297.1489, 279.1381, 251.1421	Neocryptotanshinone	Diterpenoids
P80	16.03	505.1690	$[M-H]^-$	$C_{25}H_{30}O_{11}$	505.1715	-4.95	243.0881, 241.1412, 225.0823	2'-Hydroxy-3',4'-dimethoxyisoflavan 7-*O*-*β*-*D*-glucoside 6"-*O*-acetate	Flavonoids
P81	16.13	293.1496	$[M+Na]^+$	$C_{18}H_{22}O_2$	293.1512	-5.46	265.1234, 261.1287, 257.1442, 247.1139	Miltiorolide A	Diterpenoids
P82	16.35	565.1344	$[M-H]^-$	$C_{29}H_{26}O_{12}$	565.1351	-1.24	509.0867, 323.1432, 224.0818, 211.0551	Dimethyl lithospermate	Phenolic acids
P83	16.52	521.1345	$[M-H]^-$	$C_{24}H_{26}O_{13}$	521.1301	8.44	313.0461, 141.0486	Salviaflaside	Phenolic acids
P84	18.22	313.1441	$[M-H]^-$	$C_{19}H_{22}O_4$	313.1445	-1.28	283.1308, 175.1814	Dehydrocrotonin	Diterpenoids
P85	18.41	297.1490	$[M+H]^+$	$C_{19}H_{20}O_3$	297.1485	1.61	281.1305, 279.1459, 271.1259, 241.1491	Cryptotanshinone	Diterpenoids
P86*	18.75	277.0860	$[M+H]^+$	$C_{18}H_{12}O_3$	277.0865	-1.80	263.0643, 235.1056, 231.0628, 221.0914	Tanshinone I	Diterpenoids
P87*	21.96	295.1305	$[M+H]^+$	$C_{19}H_{18}O_3$	295.1329	-8.03	281.1139, 277.1146, 263.0981, 249.1241	Tanshinone IIA	Diterpenoids
P88*	22.56	283.1670	$[M+H]^+$	$C_{19}H_{22}O_2$	283.1693	-8.12	267.1591, 225.0886, 197.1239	Miltirone	Diterpenoids
P89	22.68	319.1645	$[M+Na]^+$	$C_{20}H_{24}O_2$	319.1669	-7.52	277.0877, 249.0788, 204.0850	Saprorthoquinone	Diterpenoids
P90	24.70	367.1689	[M+Cl]-	$C_{20}H_{28}O_4$	367.1682	1.91	334.1107, 271.0346	Pinophicin A	Diterpenoids

RT: retention time; *compound with a reference standard

Table 2: Identification of the metabolite constituents of HD in plasma by UHPLC-QTOF MS

No.	RT (min)	*m/z*	Adducts	Formula	Error (ppm)	Fragment ions	Identification	Structure Type
M1	1.35	211.0612	$[M+H]^+$	$C_{10}H_{10}O_5$	5.21	195.0558, 167.0753, 105.0159	Ferulic acid-hydroxylation	Phenolic acids
M2	2.44	332.0076	$[M-H]^-$	$C_{11}H_{11}NO_9S$	-1.73	287.0819, 285.0676, 242.0637, 217.0203	Unknown	Phenolic acids
M3	2.49	226.0693	$[M+H]^+$	$C_{10}H_{11}O_5N$	-7.52	208.0462, 181.0514, 149.0384, 137.0667, 135.0412	Glycine conjugate of caffeic acid-decarbonylation-hydroxylation	Phenolic acids
M4	3.19	391.1017	$[M-H]^-$	$C_{19}H_{20}O_9$	-4.49	347.0351, 345.0284, 329.0401	Methyl-rosmarinic acid-hydration	Phenolic acids
M5	5.28	416.9955	$[M-H]^-$	$C_{18}H_{10}O_{10}S$	7.94	337.0324, 321.0465, 283.1038, 257.0786	Calycosin-dicarbonylation-dehydroxylation-sulfate	Flavonoids
M6	5.62	461.1041	$[M+H]^+$	$C_{22}H_{20}O_{11}$	-8.11	446.1054, 285.0621	Calycosin-glucuronide	Flavonoids
M7	5.63	460.1088	$[M-H]^-$	$C_{22}H_{23}NO_8S$	3.56	416.1256, 283.0624, 239.0174	Cysteine S-conjugate of calycosin-dihydrogenation	Flavonoids
M8	6.98	443.1012	$[M-H]^-$	$C_{22}H_{20}O_{10}$	6.39	267.0761, 252.0563, 208.0438	Formononetin-glucuronide	Flavonoids
M9	7.28	273.0101	$[M-H]^-$	$C_{10}H_{10}O_7S$	9.72	231.0957, 229.0707, 193.0959, 179.0928	Methyl-danshensu-dehydration-sulfate	Phenolic acids
M10	7.32	487.1294	$[M-H]^-$	$C_{24}H_{24}O_{11}$	9.88	311.0935, 283.1167, 255.1111	(6a*R*,11a*R*)-3,9,10-Tri-methoxypterocarpan-glucuronide	Flavonoids
M11	7.69	495.1550	$[M+H]^+$	$C_{23}H_{26}O_{12}$	9.70	301.0928, 213.1757, 167.0701, 57.0861	3-Hydroxy-9,10-dimethoxyptercarpan-glucuronide-hydration	Flavonoids
M12	7.99	477.1562	$[M-H]^-$	$C_{27}H_{26}O_8$	-2.29	415.0689, 321.0535, 245.0204, 224.0423	Dimethyl lithospermate-loss of $2CO_2$	Phenolic acids
M13	8.26	469.1185	$[M-H]^-$	$C_{24}H_{22}O_{10}$	9.55	293.0885, 277.0956, 257.1204, 229.0877	3α-Hydroxymethylenetanshinquinone-glucuronide	Diterpenoids
M14	9.01	286.1465	$[M+H]^+$	$C_{17}H_{19}NO_3$	9.54	256.1095, 225.1297, 213.1322	Glycine conjugate of epidanshenspiroketallactone-didecarbonylation-hydroxylation	Diterpenoids
M15	9.01	303.1563	$[M+H]^+$	$C_{18}H_{22}O_4$	-9.19	301.1411, 287.0901, 267.1429, 257.1430	Salvianonol-reduction	Diterpenoids
M16	9.10	487.1380	$[M-H]^-$	$C_{28}H_{24}O_8$	-3.78	453.0858, 399.1635	Salvianolic acid-methyl ester-dehydroxylation	Phenolic acids
M17	9.15	347.1953	$[M-H]^-$	$C_{16}H_{30}NO_7$	1.01	329.1461, 305.1073	Unknown	Phenolic acids
M18	9.15	347.1892	$[M-H]^-$	$C_{20}H_{28}O_5$	8.07	295.0911, 259.1822	Savialba acid-hydrogenation	Phenolic acids
M19	9.46	345.1734	$[M-H]^-$	$C_{20}H_{26}O_5$	7.68	301.1441, 159.1391	7-*O*-methylisomucronulatol-dimethylation-hydrogenation	Flavonoids
M20	9.55	331.1515	$[M+H]^+$	$C_{19}H_{22}O_5$	-7.55	315.0708, 313.1389, 297.1187, 295.1233	Hydroxycryptotanshinone-hydration	Diterpenoids
M21	9.56	457.1280	$[M-H]^-$	$C_{27}H_{22}O_7$	-2.79	281.0793, 265.0678, 233.0750	Unknown-glucuronide	Flavonoids
M22	9.56	458.1296	$[M-H]^-$	$C_{19}H_{25}NO_{12}$	-1.74	404.1332, 282.0887, 211.0635, 153.0436	Glycine conjugate of danshensu methyl ester-methylation-glucuronide	Phenolic acids
M23	9.71	331.1570	$[M+H]^+$	$C_{19}H_{22}O_5$	-9.06	313.1480, 297.1303, 295.1223, 277.1273	Hydroxycryptotanshinone-hydration	Diterpenoids
M24	9.88	501.1550	$[M-H]^-$	$C_{29}H_{26}O_8$	-0.98	421.1530, 245.1015, 179.1661	Dimethyl lithospermate-dehydration	Phenolic acids
M25	9.91	353.1375	$[M+H]^+$	$C_{21}H_{20}O_5$	-2.41	337.1291, 249.1284	Danshenol A-hydroxylation	Diterpenoids
M26	9.91	331.1552	$[M+H]^+$	$C_{19}H_{22}O_5$	3.62	313.1695, 295.1259, 285.1579	Hydroxycryptotanshinone-hydration	Diterpenoids
M27	9.93	346.1632	$[M+H]^+$	$C_{19}H_{23}NO_5$	-4.91	311.1239, 283.1518, 217.0991, 215.0534	Glycine conjugate of 4'-Hydroxy-5,7-dimethoxyflavan-hydrogenation	Flavonoids
M28	10.00	327.1206	$[M+H]^+$	$C_{19}H_{18}O_5$	-6.42	311.1177, 283.1185, 267.1339, 255.1285	Tanshinone IIB-hydroxylation	Diterpenoids
M29	10.00	283.0957	$[M+H]^+$	$C_{17}H_{14}O_4$	9.25	267.0869, 243.1028, 241.0864, 239.1111	Danshenxinkun A-demethylation	Diterpenoids
M30	10.01	283.0958	$[M+H]^+$	$C_{17}H_{14}O_4$	-2.42	268.0954, 239.0952, 223.0847	Formononetin-methylation	Flavonoids
M31	10.47	251.1091	$[M+H]^+$	$C_{17}H_{14}O_2$	9.73	236.1147, 233.0841, 223.1078, 219.1053, 205.0930	Dihydrotanshinone I-decarbonylation	Diterpenoids
M32	10.48	285.1125	$[M-H]^-$	$C_{17}H_{18}O_4$	-2.57	243.0406, 173.0926, 135.0734	(3*R*)-7,2',3'-Trihydroxy-4'-methoxyisoflavane-methylation-dehydroxylation	Flavonoids

Contd...

Table 2: Contd...

No.	RT (min)	*m/z*	Adducts	Formula	Error (ppm)	Fragment ions	Identification	Structure Type
M33	10.48	303.1258	$[M-H]^-$	$C_{17}H_{20}O_5$	6.61	259.0820, 241.0250, 225.0305	(*R*)-3-(5-Hydroxy-2,3,4-trimethoxyphenyl)-chroman-7-ol-decarbonylation	Flavonoids
M34	10.49	477.2654	$[M-H]^-$	$C_{30}H_{38}O_5$	1.58	459.2495, 435.1606, 415.1041	Unknown	Diterpenoids
M35	10.57	309.0750	$[M-H]^-$	$C_{18}H_{14}O_5$	-5.98	281.0871, 265.0920	3-Hydroxy-4,9-dimethoxypterocarpan-dehydration-carbonylation	Flavonoids
M36	10.65	329.1388	$[M-H]^-$	$C_{19}H_{22}O_5$	-1.97	287.1084, 285.1690, 267.0917, 257.0927	Przewalskin F-carbonylation	Diterpenoids
M37	10.76	295.0980	$[M+H]^+$	$C_{18}H_{14}O_4$	5.13	279.1138, 277.0825,267.1074, 265.0970	Dihydrotanshinone I-hydroxylation	Diterpenoids
M38	10.76	489.1742	$[M-H]^-$	$C_{25}H_{30}O_{10}$	-4.95	313.1620, 149.0526	Neocryptotanshinone-glucuronide	Diterpenoids
M39	10.78	475.1952	$[M+H]^+$	$C_{25}H_{30}O_9$	-2.23	299.1636, 281.1463, 193.1597	Normiltirone-glucuronide	Diterpenoids
M40	10.82	247.0953	$[M+H]^+$	$C_{14}H_{14}O_4$	-4.80	233.0709,231.0961, 229.0855, 189.0628	(6a*R*,11a*R*)-3,9-Dimethoxy-10-hydroxypterocarpan- demethylation-decarbonylation-hydroxylation	Flavonoids
M41	10.83	470.1298	$[M-H]^-$	$C_{24}H_{25}NO_7S$	4.05	416.0904, 311.1240	N-acetylcysteine S conjugate of 17-Hydroxycryptotanshinone	Diterpenoids
M42	11.14	318.1481	$[M+H]^+$	$C_{21}H_{19}NO_2$	-2.37	304.1107, 300.0863, 278.1487	Salviadione-methylation-carbonylation-dehydroxylation	Diterpenoids
M43	11.24	331.1883	$[M+H]^+$	$C_{20}H_{26}O_4$	-6.30	316.1387, 315.1490, 313.1725, 299.1958, 284.1378	Microstegiol-hydroxylation	Diterpenoids
M44	11.25	459.1616	$[M+H]^+$	$C_{24}H_{26}O_9$	-7.32	311.0986, 237.1277	3-Hydroxytanshinone IIB-glu	Diterpenoids
M45	11.66	455.1342	$[M-H]^-$	$C_{24}H_{24}O_9$	-1.22	279.1132, 263.1598, 199.0646	Danshenxinkun B-glucuronide	Diterpenoids
M46	11.67	455.1354	$[M-H]^-$	$C_{24}H_{24}O_9$	1.42	279.1048, 249.0947, 211.1134	Trijuganone B-glucuronide	Diterpenoids
M47	11.78	455.1349	$[M-H]^-$	$C_{24}H_{24}O_9$	0.32	441.1393, 425.1377	Calycosin 7-*O*-*β*-*D*-glucoside-6''-*O*-acetate-dehydroxylation	Flavonoids
M48	11.80	285.1513	$[M+H]^+$	$C_{18}H_{20}O_3$	9.75	267.1340, 241.1364, 229.0932,	Deoxyneocryptotanshinone-demethylation	Diterpenoids
M49	11.82	311.1285	$[M+H]^+$	$C_{19}H_{18}O_4$	2.30	295.1448, 293.1273, 265.1226, 249.0917	Danshenxinkun A-methylation	Diterpenoids
M50	11.82	329.1389	$[M+H]^+$	$C_{19}H_{20}O_5$	1.67	311.1154, 269.1005, 267.1443, 239.1102	Tanshinone IIB-hydration	Diterpenoids
M51	11.84	311.1294	$[M+H]^+$	$C_{19}H_{18}O_4$	5.19	296.1383, 295.1222, 293.0733, 283.1355	Danshenxinkun A-methylation	Diterpenoids
M52	11.93	329.1378	$[M+H]^+$	$C_{19}H_{20}O_5$	-1.67	311.1168, 283.1365, 267.1186	Tanshinone IIB-hydration	Diterpenoids
M53	11.86	347.0910	$[M+H]^+$	$C_{21}H_{14}O_5$	-1.15	301.0718, 203.0743, 163.0736	Monodydroxytanshinone I-methylation-dicarbonylation-dehydroxylation	Diterpenoids
M54	11.97	357.1350	$[M-H]^-$	$C_{20}H_{22}O_6$	1.79	329.1602, 313.1465, 299.1015	Neocryptotanshinone-carboxylation	Diterpenoids
M55	12.48	455.1375	$[M-H]^-$	$C_{24}H_{24}O_9$	6.03	279.1034, 265.1148, 261.0883, 251.1161	Trijuganone B-glucuronide	Diterpenoids
M56	12.48	456.1505	$[M-H]^-$	$C_{20}H_{27}NO_{11}$	-1.39	412.0751, 375.0837, 279.1235	N-acetylcysteine S conjugate of methyl rosmarinate	Phenolic acids
M57	12.60	441.1738	$[M-H]^-$	$C_{21}H_{30}O_{10}$	-6.39	299.1807, 265.1354	(3*R*, 4*R*)-4, 7-hydroxy-2', 3'-dimethoxyisoflavane-4'-*O*-*β*-*D*-glucoside-decarbonylation-hydration	Flavonoids
M58	12.93	351.1078	$[M+H]^+$	$C_{17}H_{18}O_8$	1.01	335.1120, 307.0831, 297.068, 199.0493	4'-Hydroxy-5,7-dimethoxyflavan-hydroxylation	Flavonoids
M59	12.95	325.1166	$[M-H]^-$	$C_{12}H_{22}O_{10}$	7.93	311.1232, 282.1309, 265.0908	Unknown	Diterpenoids
M60	12.95	327.1227	$[M-H]^-$	$C_{19}H_{20}O_5$	-3.35	285.1346, 241.1055	7-*O*-methylisomucronulatol-carbonylation-dehydroxylation	Flavonoids
M61	12.95	281.1205	$[M-H]^-$	$C_{18}H_{18}O_3$	7.76	265.0982, 261.1283, 251.0887, 239.1044	Przewalskin F-reduction	Diterpenoids
M62	13.58	297.1123	$[M-H]^-$	$C_{18}H_{18}O_4$	-3.14	253.0741, 179.0598	4'-Hydroxy-5,7-dimethoxyflavan-carbonylation-dehydroxylation	Flavonoids
M63	13.86	251.1427	$[M+H]^+$	$C_{18}H_{18}O$	-1.36	239.1393, 235.1523, 233.1370, 223.1133	Cryptotanshinone-dehydration-decarbonylation	Diterpenoids

Contd...

Table 2: Contd...

No.	RT (min)	*m/z*	Adducts	Formula	Error (ppm)	Fragment ions	Identification	Structure Type
M64	13.86	237.0921	$[M+H]^+$	$C_{16}H_{12}O_2$	4.61	223.1107, 209.0947, 205.0989, 194.0785	Danshenxinkun C-dehydroxylation	Diterpenoids
M65	13.87	449.0588	$[M-H]^-$	$C_{20}H_{18}O_{10}S$	8.93	415.0845, 407.0618, 405.0615, 359.0374	Methyl rosmarinate-dehydration-methylation-sulfate	Phenolic acids
M66	13.87	413.0883	$[M-H]^-$	$C_{21}H_{18}O_9$	1.20	345.1053, 323.0604, 295.0321, 223.0262	Methyl rosmarinate-dicarbonylation-dehydroxylation	Phenolic acids
M67	13.87	459.0896	$[M-H]^-$	$C_{22}H_{20}O_{11}$	-8.03	415.0881, 341.1108	Kaempferol 3-*O*-*β*-*D*-glucoside-carbonylation-dehydroxylation	Flavonoids
M68	14.15	381.1351	$[M-H]^-$	$C_{22}H_{22}O_6$	1.94	375.1008, 271.1079	Calycosin-7-*O*-*β*-*D*-glucoside-dehydroxylation	Flavonoids
M69	15.79	443.1146	$[M-H]^-$	$C_{26}H_{20}O_7$	2.20	425.1021, 367.0838, 285.0845, 275.0290	Unknown	Flavonoids
M70	20.29	261.0899	$[M+H]^+$	$C_{18}H_{12}O_2$	-4.24	246.0793, 233.1012, 219.0659, 205.0969	Tanshinone I-dehydroxylation	Diterpenoids
M71	20.30	325.1461	$[M+H]^+$	$C_{20}H_{20}O_4$	8.19	281.1305, 279.0786, 261.0901, 253.1611	Dehydromiltirone-carboxylation	Diterpenoids
M72	20.64	299.1276	$[M+H]^+$	$C_{18}H_{18}O_4$	-0.62	284.0908, 281.1136, 191.1415, 141.0617	15,16-Dihydrotanshinol B-dehydroxylation	Diterpenoids
M73	21.74	293.1421	$[M+H]^+$	$C_{19}H_{18}NO_2$	3.65	277.0615, 269.0408, 235.0188	Salviadione-dehydrogenation	Diterpenoids
M74	22.24	341.1925	$[M+H]^+$	$C_{18}H_{28}O_6$	-9.86	307.1255, 299.1614, 241.1284, 165.1307	Militibetin A-hydration-dihydroxylation	Diterpenoids

RT: retention time

compounds, including dehydration, sulfation, methylation, and hydroxylation.

Identification of terpenoids

A total of 84 terpenoid-related compounds were detected on HD after oral administration, which included diterpenoids and triterpenoid saponins. Tanshinones are the main diterpenoids *in vivo* and exhibit various bioactivities, such as anti-cancer and anti-pulmonary fibrosis activities.[26,27]

According to a comprehensive analysis of the chemical composition of HD, tanshinones usually show a high response in the positive mode, and the most obvious feature of these compounds is the neutral loss of CO and H_2O. Taking P30 ($C_{19}H_{20}O_4$) as an example, the protonated $[M + H]^+$ ion was observed at m/z 313.1431. The characteristic information exhibited at m/z 297.1280 ($[M + H\text{-}O]^+$), 295.1333 ($[M + H\text{-}H_2O]^+$), 285.1468 ($[M + H\text{-}CO]+$), and 271.1060 ($[M + H\text{-}CO\text{-}CH_2]^+$), which was considered to be hydroxycryptotanshinone.[28] P67 (*m*/z 297.1116, $[M + H]^+$) produced a molecular formula of $C_{18}H_{16}O_4$, while the characteristic fragment ions at m/z 281.1041 ($[M + H\text{-}O]^+$), 279.1038 ($[M + H\text{-}H_2O]^+$), 263.0995 ($[M + H\text{-}H_2O\text{-}O]^+$), and 251.1018 ($[M + H\text{-}H_2O\text{-}CO]^+$) in MS^2 information. Therefore, P67 was identified as danshenxinkun A by comparison with the standard.

Metabolite M49 ($C_{19}H_{18}O_4$) presented a quasi-molecular ion at m/z 311.1285 ($[M + H]^+$), corresponding to CH_2 from P67. A range of unique fragment information were collected at m/z 295.1448 ($[M + H\text{-}O]^+$), 293.1273 ($[M + H\text{-}H_2O]^+$), 265.1226 ($[M + H\text{-}H_2O\text{-}CO]^+$), and 249.0917 ($[M + H\text{-}H_2O\text{-}CO]^+$). Therefore, M49 was speculated to be methyl-danshexinkun A [Figure 6]. M20 and M23 exhibited $[M + H]^+$ ions at m/z 331.1515 and 331.1570, respectively, which confirmed the same molecular formula as $C_{19}H_{18}O_5$. MS^2 information was obtained at m/z 313, 297, and 295, which indicated losses of 18 Da (-H_2O), 28 Da (-CO), and 36 Da (-2H_2O), respectively. The quasi-molecular ions were 18 Da larger than P30, suggesting that they may be the hydration products of P30. Hydroxylation, dehydroxylation, decarbonylation, methylation, hydration, and other reactions occur during terpenoid metabolism.

DISCUSSION

In this study, HD-related metabolic profiling was used to systematically characterize the absorbed compounds and their products. In total, 90 prototypes and 74 biochemical products were identified in rats orally administered HD. The major components found in rats were flavonoids, phenolic acids, and terpenoids, indicating that these could be the potential bioactive components of HD.

Flavonoids are the main active components of Huangqi and are highly bioavailable and easily absorbed into the blood. Calycosin, the aglycone of calycosin-7-*O*-*β*-*D*-glucoside, which possessed pharmacological activities, including anti-inflammatory and anti-hepatic injury effects.[29,30] Calycosin-7-*O*-*β*-*D*-glucoside may lose a glucosyl group into calycosin and produced formononetin by dehydroxylation reaction. Calycosin can be metabolized by glucuronidation to produce calycosin-glucuronide metabolites with improved bioavailability. In addition, two isoflavone glycosides (calycosin

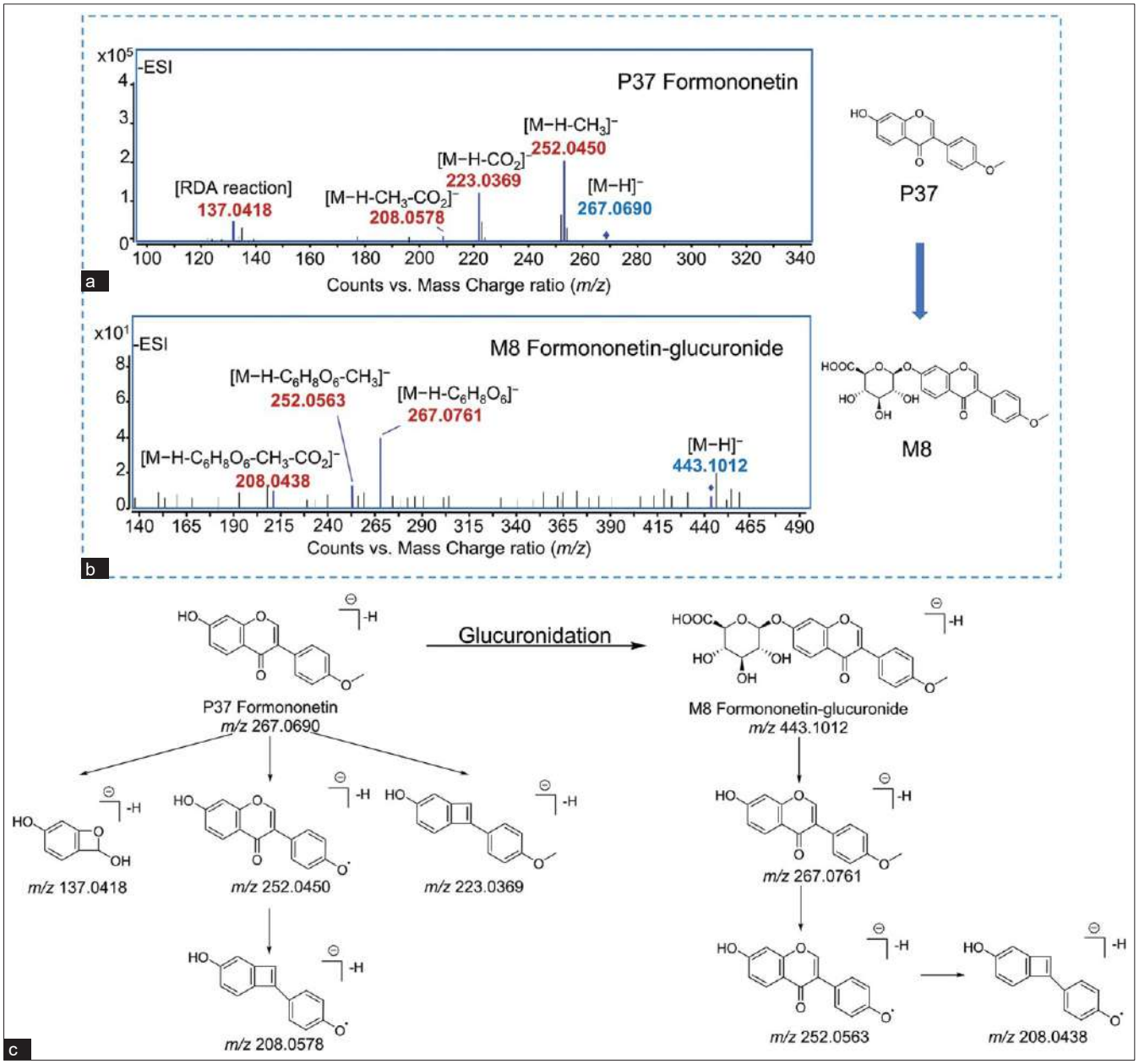

Figure 3: The MS/MS spectra of formononetin and its possible metabolite. (a) Formononetin; (b) Formononetin-glucuronidation; (c) Possible fragment pathways

7-*O*-*β*-*D*-glucoside-6''-*O*-acetate and formononetin 7-*O*-*β*-*D*-glucoside-6"-*O*-malonate) and a flavonoid glycoside (odoratin 7-*O*-*β*-D-glucopyranoside) were detected, demonstrating that they could be directly absorbed *in vivo*. According to the metabolic information, glucuronidation and cysteine S-conjugation are the major metabolic pathways. Some Phase I reactions, such as methylation, hydroxylation, dehydroxylation, and reduction, occurred during the metabolism of HD.

The plasma that contained the medication had prototypical components and phenolic acid metabolites in it. With pharmacological characteristics including antithrombotic actions, the one-phenolic acid molecule known as danshensu is a powerful physiologically active chemical. [31] in Danshensu takes up residence in the enters the circulation and, by means of a dehydration process, generates caffeic acid; this acid may then be methylated to create caffeic acid methyl ester. It is via glycine conjugation processes, glucuronidation, sulfation, and methylation that Danshensu produces metabolites. Researching and characterizing the pertinent biotransformation products in rats that mostly experienced Phase II metabolic processes was based on these findings.

Terpenoids, including diterpenoids and triterpenoids, are the most abundant compounds found in drug-containing plasma. A total of 84 terpenoids were identified *in vivo* during HD, including 46 parent constituents and 38 metabolites. Tanshinones are the main diterpenoids found in Danshen. Cryptotanshinone is easily metabolized into tanshinone IIB,

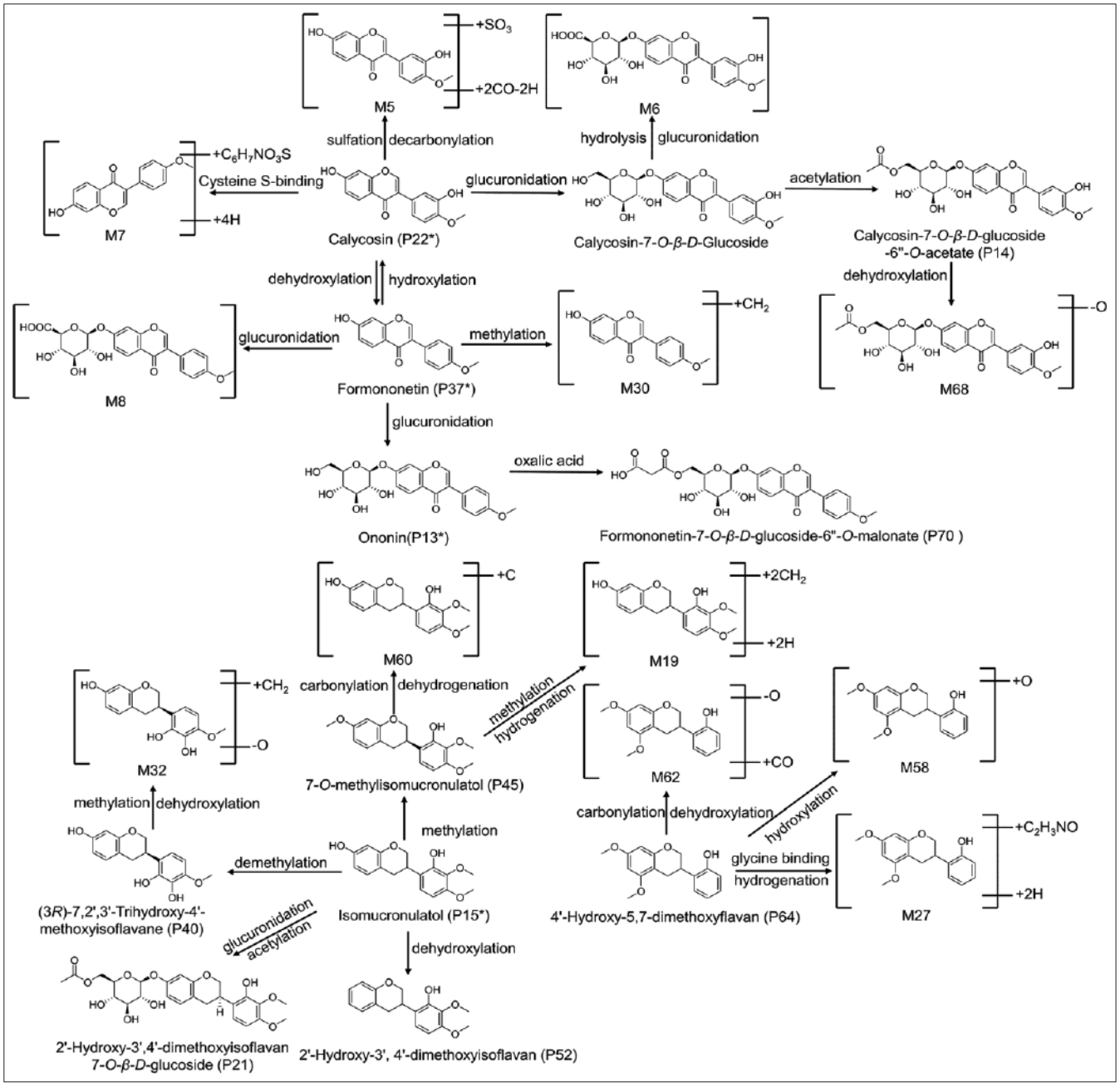

Figure 4: Proposed metabolic pathways of some typical flavonoids in rat plasma after oral administration of Huangqi-Danshen

hydroxycryptotanshinone, and tanshinone I. Tanshinone IIB and hydroxycryptotanshinone can further form metabolites through hydration reactions. Tanshinone I is metabolized to danshexinkun A, which generates methylated metabolites. Saponins are generally recognized to have poor oral bioavailability. A related study of Huangqi *in vitro* shows that it contains a large amount of triterpene saponins,[32] but during *in vivo* metabolism, triterpene saponin compounds enter the blood to a lesser extent. In our study, isoastragaloside IV was the only triterpene saponin-related component detected in rat plasma. This may be due to the large relative molecular mass of the triterpenoid saponin constituents, which makes it more difficult for them to be absorbed *in vivo*, resulting in low bioavailability.

As mentioned above, the absorbed components mainly consist of flavonoids, phenolic acids, and terpenoids, suggesting that these components are the major contributors to HD. A large number of multi-step metabolites were found in plasma, indicating that these HD compounds underwent abundant metabolic reactions *in vivo*. Therefore, conducting an in-depth and comprehensive metabolic process analysis of HD in combination with biological samples such as urine, tissue, and feces is necessary.

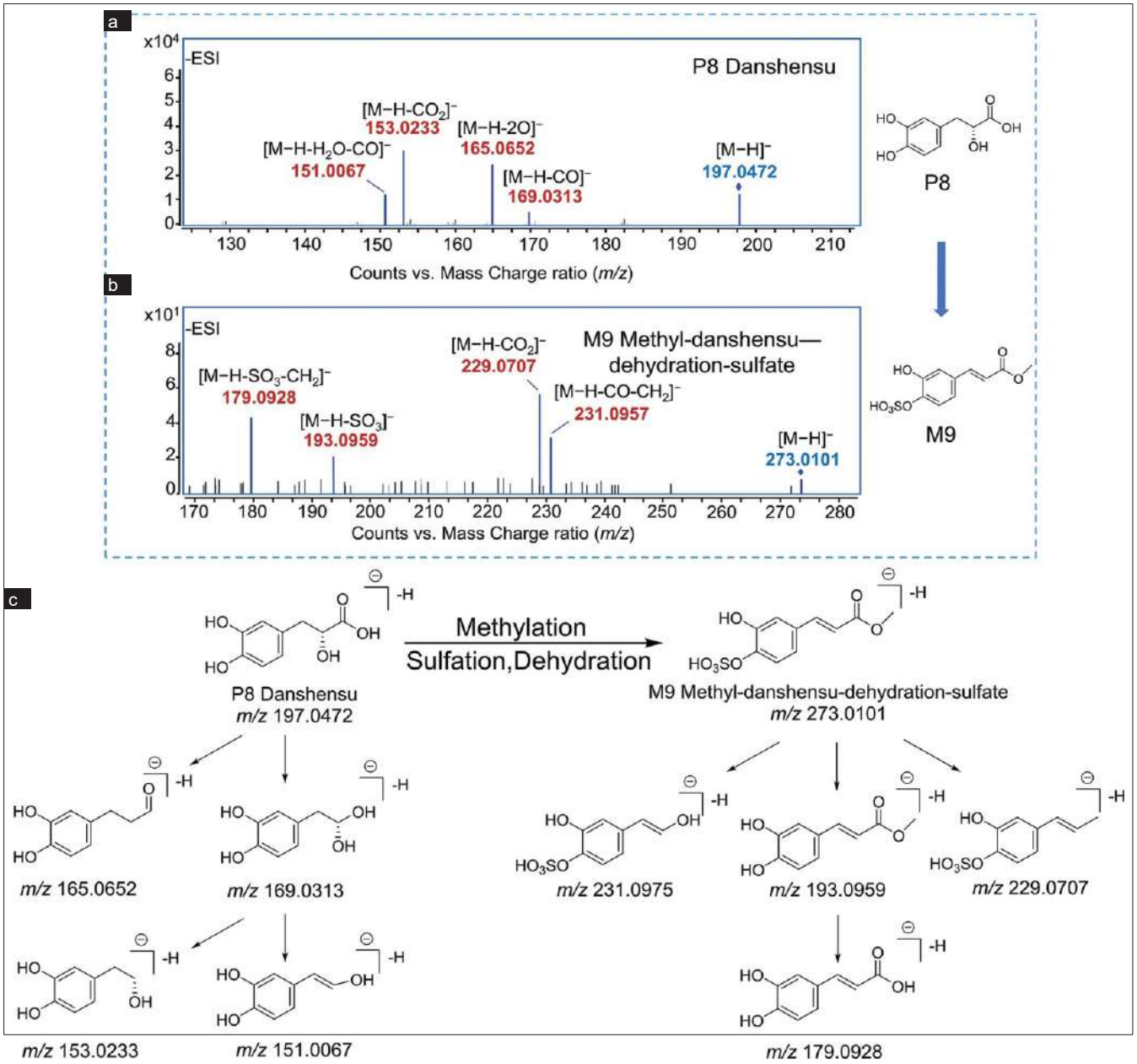

Figure 5: The MS/MS spectra of Danshensu and its possible metabolite. (a) Danshensu; (b) Methyl-danshensu-dehydration-sulfate; (c) Possible fragment

This study aimed to elucidate the pharmacodynamic underpinnings of HD and offer a scientific foundation for the sensible use of this drug in clinical research and associated new drug development.

Conclusions

In vivo, TCMs may be subjected to a wide variety of drug metabolic mechanisms. By shedding or binding groups, the prototypes absorbed in biological matrices are transformed into metabolites. Metabolites in close proximity to one another also undergo biotransformation. Manual processing of mass discrepancies is required by traditional metabolite identification methodologies. between distinctive ions, a process that is both tedious and time-consuming. One way to lessen the burden on data processors is to automate the calculation of the mass difference using R programming. Based on the mass differences between prototypes and their products using UHPLC-QTOF MS, this work developed a systematic technique to identify and profile the exogenous components in TCMs. Both potential prototype components and metabolites that underwent multistage reactions were effectively screened using this technique. This led to the discovery of 164 chemicals in rat plasma, including 90 prototypes and 74 metabolites. Terpenoids, phenolic acids, and flavonoids are its primary constituents. In vivo component characterization of HD has established

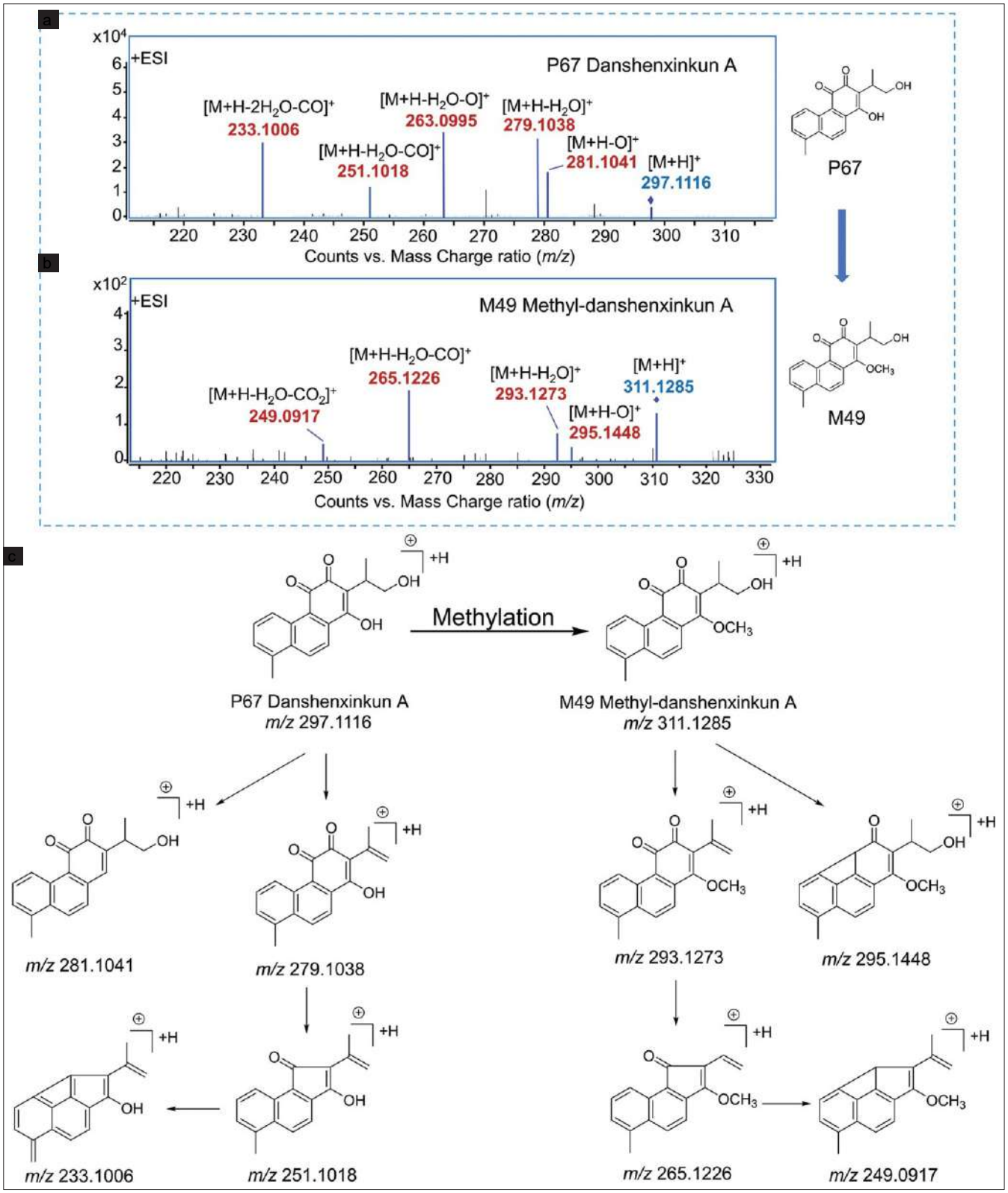

Figure 6: The MS/MS spectra of Danshenxinkun A and its possible metabolite. (a) Danshenxinkun A; (b) Methyl-danshenxinkun A; (c) Possible fragment pathways

for elucidating its active ingredient groups against diseases. Simultaneously, this strategy may provide a feasible method for metabolic profiling of exogenous compounds in biological matrices.

References

1. Kainuma M, Kawakatsu S, Kim JD, Ouma S, Iritani O, Yamashita KI, *et al*. Metabolic changes in the plasma of mild Alzheimer's disease patients treated with Hachimijiogan. Front Pharmacol 2023;14:1203349.
2. Han Y, Sun H, Zhang A, Yan G, Wang XJ. Chinmedomics, a new strategy for evaluating the therapeutic efficacy of herbal medicines. Pharmacol Ther 2020;216:107680.
3. Tang XY, Zeng JX, Dai ZQ, Chen MH, Ye MN, Yao ZH, *et al*. Identification and characterization of chemical constituents in Qi-Lin pills and their metabolites in rat bio-samples after oral administration using ultra-high performance liquid chromatography with quadrupole time-of-flight mass spectrometry. J Pharm Biomed Anal 2020;188:113402.
4. Zhang X, Liao M, Cheng X, Liang C, Diao X, Zhang L. Ultrahigh-performance liquid chromatography coupled with triple quadrupole and time-of-flight mass spectrometry for the screening and identification of the main flavonoids and their metabolites in rats after oral administration of *Cirsium japonicum* DC. extract. Rapid Commun Mass Spectrom 2018;32:1451-61.
5. Lai H, Ouyang Y, Tian G, Zhao J, Zhang J, Zhang J, *et al*. Rapid characterization and identification of the chemical constituents and the metabolites of Du-zhi pill using UHPLC coupled with quadrupole time-of-flight mass spectrometry. J Chromatogr B Analyt Technol Biomed Life Sci 2022;1209:123433.
6. Li BX, Li PY, Hao LX, Xue XX, Kong SS, Zhao QH, *et al*. Identification and determination of the major constituents in XieBaiSan by ultraperformance liquid chromatography – Mass spectrometry. World J Tradit Chin Med 2024;10:334-46.
7. Huang AX, Li JM, Yang L, Chen L, Zhou ZH, Li P, *et al*. A mass defect filtering combined background subtraction strategy for rapid screening and identification of metabolites in rat plasma after oral administration of Yindan Xinnaotong soft capsule. J Pharm Biomed Anal 2023;231:115400.
8. Shi XJ, Yang WZ, Qiu S, Yao CL, Shen Y, Pan HQ, *et al*. An in-source multiple collision-neutral loss filtering based nontargeted metabolomics approach for the comprehensive analysis of malonyl-ginsenosides from *Panax ginseng*, *P. quinquefolius*, and *P. notoginseng*. Anal Chim Acta 2017;952:59-70.
9. Yuan S, Gao P, Shi Y, Tu P, Jiang Y. Rapid screening and identification of metabolites of murpanicin in rats by UHPLC/Q-TOF-MS/MS combined with diagnostic fragment ions (DFIs) and multiple mass defect filter. J Pharm Biomed Anal 2022;213:114679.
10. Zeng SL, Duan L, Chen BZ, Li P, Liu EH. Chemicalome and metabolome profiling of polymethoxylated flavonoids in citri reticulatae pericarpium based on an integrated strategy combining background subtraction and modified mass defect filter in a Microsoft excel platform. J Chromatogr A 2017;1508:106-20.
11. Albóniga OE, González O, Alonso RM, Xu Y, Goodacre R. Optimization of XCMS parameters for LC-MS metabolomics: An assessment of automated versus manual tuning and its effect on the final results. Metabolomics 2020;16:14.
12. Riquelme G, Zabalegui N, Marchi P, Jones CM, Monge ME. A python-based pipeline for preprocessing LC-MS data for untargeted metabolomics workflows. Metabolites 2020;10:416.
13. Wang L, Ye H, Sun D, Meng T, Cao L, Wu M, *et al*. Metabolic pathway extension approach for metabolomic biomarker identification. Anal Chem 2017;89:1229-37.
14. Djoumbou-Feunang Y, Fiamoncini J, Gil-de-la-Fuente A, Greiner R, Manach C, Wishart DS. BioTransformer: A comprehensive computational tool for small molecule metabolism prediction and metabolite identification. J Cheminform 2019;11:2.
15. Li XL, Guo ZF, Wen XD, Li MN, Yang H. A molecular networking-assisted automatic database screening strategy for comprehensive annotation of small molecules in complex matrices. J Chromatogr A 2023;1710:464417.
16. Zhang CH, Yang X, Wei JR, Chen NM, Xu JP, Bi YQ, *et al*. Ethnopharmacology, phytochemistry, pharmacology, toxicology and clinical applications of radix astragali. Chin J Integr Med 2021;27:229-40.
17. Kong X, Wang F, Niu Y, Wu X, Pan Y. A comparative study on the effect of promoting the osteogenic function of osteoblasts using isoflavones from radix *Astragalus*. Phytother Res 2018;32:115-24.
18. Ding X, Lv J, Luan J, Zhang J. Calycosin may alleviate Ang II-induced pro-proliferative effects on glomerular mesangial cells via partially inhibiting autophagy and ERK signaling pathway. Biol Pharm Bull 2020;43:1893-8.
19. Yang L, Han X, Xing F, Wu H, Shi H, Huang F, *et al.* Total flavonoids of *Astragalus* attenuates experimental autoimmune encephalomyelitis by suppressing the activation and inflammatory responses of microglia via JNK/AKT/NFκB signaling pathway. Phytomedicine 2021;80:153385.
20. Liu LJ, Li HF, Xu F, Wang HY, Zhang YF, Liu GX, *et al.* Exploring the *in vivo* existence forms (23 original constituents and 147 metabolites) of astragali radix total flavonoids and their distributions in rats using HPLC-DAD-ESI-IT-TOF-MS(n). Molecules 2020;25:5560.
21. Zhou G, Zhu J, Jin L, Chen J, Xu R, Zhao Y, *et al*. Salvianolic-acid-B-loaded HA self-healing hydrogel promotes diabetic wound healing through promotion of anti-inflammation and angiogenesis. Int J Mol Sci 2023;24:6844.
22. Lee HG, Kwon S, Moon SK, Cho SY, Park SU, Jung WS, *et al*. Neuroprotective effects of Geopung-Chunghyuldan based on its salvianolic acid B content using an *in vivo* stroke model. Curr Issues Mol Biol 2023;45:1613-26.
23. Cao LJ, Xie HT, Chu ZX, Ma Y, Wang MM, Zhuang S. Protective effect of Shenfu injection against sepsisinduced acute lung injury by suppressing inflammation and apoptosis through the regulation of the Janus kinase 2/signal transducer and activator of transcription 3 pathway. World J Tradit Chin Med 2024;10:528-34.
24. Choi HG, Tran PT, Lee JH, Min BS, Kim JA. Anti-inflammatory activity of caffeic acid derivatives isolated from the roots of *Salvia miltiorrhiza* bunge. Arch Pharm Res 2018;41:64-70.
25. Mi N, Cheng T, Li H, Yang P, Mu X, Wang X, *et al*. Metabolite profiling of traditional Chinese medicine formula Dan Zhi tablet: An integrated strategy based on UPLC-QTOF/MS combined with multivariate statistical analysis. J Pharm Biomed Anal 2019;164:70-85.
26. Schaf J, Shinhmar S, Zeng Q, Pardo OE, Beesley P, Syed N, *et al*. Enhanced sestrin expression through tanshinone 2A treatment improves PI3K-dependent inhibition of glioma growth. Cell Death Discov 2023;9:172.
27. He X, Zhong Z, Wang Q, Jia Z, Lu J, Chen J, *et al*. Pharmacokinetics and tissue distribution of bleomycin-induced idiopathic pulmonary fibrosis rats treated with cryptotanshinone. Front Pharmacol 2023;14:1127219.
28. Gong L, Xu H, Yuan H, Wang L, Yin X, Fan M, *et al*. Identification

of absorbed constituents and evaluation of the pharmacokinetics of main compounds after oral administration of yindanxinnaotong by UPLC-Q-TOF-MS and UPLC-QqQ-MS. RSC Adv 2018;8:15725-39.
29. Su X, Huang Q, Chen J, Wang M, Pan H, Wang R, *et al*. Calycosin suppresses expression of pro-inflammatory cytokines via the activation of p62/Nrf2-linked heme oxygenase 1 in rheumatoid arthritis synovial fibroblasts. Pharmacol Res 2016;113:695-704.
30. Duan X, Meng Q, Wang C, Liu Z, Liu Q, Sun H, *et al*. Calycosin attenuates triglyceride accumulation and hepatic fibrosis in murine model of non-alcoholic steatohepatitis via activating farnesoid X receptor. Phytomedicine 2017;25:83-92.
31. Xue Y, Zhang L, Zhang L, Sun W, Fang Z, Leng Y, *et al*. Danshensu prevents thrombosis by inhibiting platelet activation via SIRT1/ROS/mtDNA pathways without increasing bleeding risk. Phytomedicine 2022;104:154271.
32. Huang J, Chen H, Li C, Liu W, Ma W, Rui W. Screening and identification of the metabolites of water extracts of raw and honey-processed *Astragalus* in rat urine based on UHPLC/ESI-Q-TOF-MS and multivariate statistical analysis. J Am Soc Mass Spectrom 2018;29:1919-35.